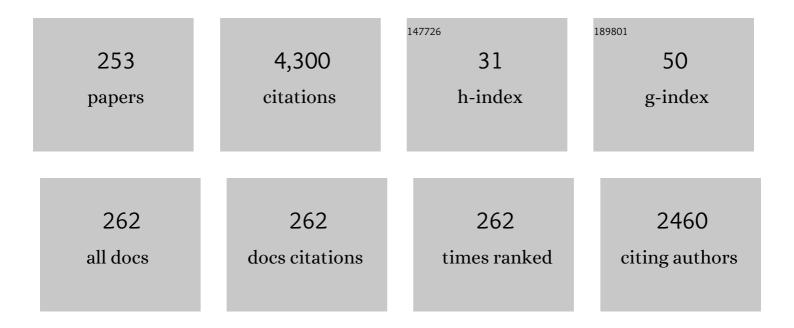
List of Publications by Year in descending order

Source: https://exaly.com/author-pdf/5284578/publications.pdf Version: 2024-02-01



#	Article	IF	CITATIONS
1	Influence of elevated temperature and reduced pressure on the degradation of iron nitride compound layer formed by plasma nitriding in <scp>AISI D2</scp> tool steels. Engineering Reports, 2022, 4, e12371.	0.9	0
2	Effect of nitriding preâ€treatment on the tribocorrosion behavior of physical vapor depositionâ€coated tool steel. Engineering Reports, 2022, 4, e12382.	0.9	0
3	Sliding wear behavior of duplex coatings with different plasma nitride layers and a <scp>Crâ€Alâ€Tiâ€Bâ€N</scp> coating. Engineering Reports, 2022, 4, e12377.	0.9	4
4	Tailoring Nonmetallic Inclusions in 42CrMo4 as a Preparative Tool for Active and Reactive Steel Melt Filtration. Advanced Engineering Materials, 2022, 24, 2100640.	1.6	8
5	Manufacture of carbon-bonded alumina based on a lactose-tannin binder system via slip casting. Ceramics International, 2022, 48, 148-156.	2.3	9
6	Experimental and Numerical Investigation of High-Temperature Multi-Axial Fatigue. Journal of Engineering for Gas Turbines and Power, 2022, 144, .	0.5	1
7	Deformation behaviour of TWIP steels: Constitutive modelling informed by local and integral experimental methods used in concert. Materials Characterization, 2022, 184, 111667.	1.9	9
8	Deformation Lenses in a Bonding Zone of High-Alloyed Steel Laminates Manufactured by Cold Roll Bonding. Metals, 2022, 12, 590.	1.0	0
9	Microstructural evolution of the bonding zone in TRIP-TWIP laminate produced by accumulative roll bonding. Materials Science & Engineering A: Structural Materials: Properties, Microstructure and Processing, 2022, 840, 142866.	2.6	5
10	Non-cube-on-cube orientation relationship between M23C6 and austenite in an austenitic stainless steel. Scripta Materialia, 2022, 213, 114597.	2.6	11
11	Planarâ€biaxial lowâ€cycle fatigue behavior of the nickelâ€base alloy Inconel 718 at elevated temperatures under selected loading conditions. Fatigue and Fracture of Engineering Materials and Structures, 2022, 45, 1571-1586.	1.7	1
12	Effect of N2–H2 Ratio during Conventional Plasma Nitriding of Intermetallic FeAl40 Alloy on Electrochemical Corrosion Parameters in Sulphuric Acid. Metals, 2022, 12, 649.	1.0	1
13	Nitriding behaviour of the intermetallic alloy FeAl. International Journal of Materials Research, 2022, 96, 781-786.	0.1	1
14	Highâ€Temperature Ternary Oxide Phases in Tantalum/Niobium–Alumina Composite Materials. Advanced Engineering Materials, 2022, 24, .	1.6	6
15	Highâ€Temperature Compressive Behavior of Refractory Alumina–Niobium Composite Material. Advanced Engineering Materials, 2022, 24, .	1.6	8
16	Coarseâ€Grained Refractory Composite Castables Based on Alumina and Niobium. Advanced Engineering Materials, 2022, 24, .	1.6	7
17	Novel method for in situ damage monitoring during ultrasonic fatigue testing by the advanced acoustic emission technique. International Journal of Fatigue, 2021, 142, 105918.	2.8	18
18	Ultrafine-grained CrMnNi steels: Lueders phenomenon and texture inheritance. Materials Science & Engineering A: Structural Materials: Properties, Microstructure and Processing, 2021, 799, 140197.	2.6	9

#	Article	IF	CITATIONS
19	Fatigue of carburised CrNiMo steel: Testing and modelling concept. Fatigue and Fracture of Engineering Materials and Structures, 2021, 44, 788-804.	1.7	5
20	Manufacturing Fe–TiC Composite Powder via Inert Gas Atomization by Forming Reinforcement Phase In Situ. Advanced Engineering Materials, 2021, 23, 2000717.	1.6	10
21	Effect of Nitriding Potential KN on the Formation and Growth of a "White Layer―on Iron Aluminide Alloy. Metallurgical and Materials Transactions B: Process Metallurgy and Materials Processing Science, 2021, 52, 414-424.	1.0	10
22	The role of grain size in static and cyclic deformation behaviour of a laser reversion annealed metastable austenitic steel. Fatigue and Fracture of Engineering Materials and Structures, 2021, 44, 43-62.	1.7	5
23	Review on Strain Localization Phenomena Studied by Highâ€Resolution Digital Image Correlation. Advanced Engineering Materials, 2021, 23, 2001409.	1.6	19
24	Impact of high temperature on the compression behavior of carbon-bonded alumina filters with functionalized coatings. Ceramics International, 2021, 47, 3920-3927.	2.3	5
25	Review on Strain Localization Phenomena Studied by Highâ€Resolution Digital Image Correlation. Advanced Engineering Materials, 2021, 23, 2170011.	1.6	13
26	Aluminum-alloyed lightweight stainless steels strengthened by B2-(Ni,Fe)Al precipitates. Materials and Design, 2021, 206, 109813.	3.3	6
27	Effects of Plasma-Chemical Composition on AISI 316L Surface Modification by Active Screen Nitrocarburizing Using Gaseous and Solid Carbon Precursors. Metals, 2021, 11, 1411. In situ characterization of the functional degradation of a <mml:math< td=""><td>1.0</td><td>6</td></mml:math<>	1.0	6
28	xmlns:mml="http://www.w3.org/1998/Math/MathML" altimg="si1.svg"> <mml:mrow><mml:mo>[</mml:mo><mml:mrow><mml:mn>00</mml:mn><mml:mover accent="true"><mml:mn>1</mml:mn><mml:mo>Â⁻</mml:mo></mml:mover </mml:mrow><mml:mo>]orientated Fe–Mn–Al–Ni single crystal under compression using acoustic emission measurements.</mml:mo></mml:mrow>	no>∛¦mml	:mrow>
29	Acta Materialia, 2021, 220, 117333. Acoustic emission measurements on metastable austenitic steel oligocrystals. Materials Science & Engineering A: Structural Materials: Properties, Microstructure and Processing, 2021, 827, 142066.	2.6	4
30	Direct tuning of the microstructural and mechanical properties of high-alloy austenitic steel by electron beam melting. Additive Manufacturing, 2021, 47, 102253.	1.7	1
31	The fatigue life of 42CrMo4 steel in the range of HCF to VHCF at elevated temperatures up to 773 K. International Journal of Fatigue, 2021, 152, 106437.	2.8	3
32	Very High Cycle Fatigue Investigations on the Fatigue Strength of Additive Manufactured and Conventionally Wrought Inconel 718 at 873 K. Metals, 2021, 11, 1682.	1.0	9
33	Influence of Oxygen Admixture on Plasma Nitrocarburizing Process and Monitoring of an Active Screen Plasma Treatment. Applied Sciences (Switzerland), 2021, 11, 9918.	1.3	4
34	Synthesis of Niobium-Alumina Composite Aggregates and Their Application in Coarse-Grained Refractory Ceramic-Metal Castables. Materials, 2021, 14, 6453.	1.3	11
35	Influence of C and N on Strain-Induced Martensite Formation in Fe-15Cr-7Mn-4Ni-0.5Si Austenitic Steel. Materials, 2021, 14, 6502.	1.3	7
36	Cyclic Crack Growth in Chemically Tailored Isotropic Austenitic Steel Processed by Electron Beam Powder Bed Fusion. Materials, 2021, 14, 6544.	1.3	0

#	Article	IF	CITATIONS
37	Influence of Carbon Nanotubesâ€Based Coatings on the Highâ€Temperature Compression Strength of Al 2 O 3 Foam Filter Structures. Advanced Engineering Materials, 2020, 22, 1900423.	1.6	3
38	Effect of Filter Functional Coating on Detrimental Nonmetallic Inclusions in 42CrMo4 Steel and Its Resulting Mechanical Properties. Advanced Engineering Materials, 2020, 22, 1900540.	1.6	8
39	Influence of the local degree of deformation on the temperature dependent fatigue behaviour of a ferritic–pearlitic steel. Fatigue and Fracture of Engineering Materials and Structures, 2020, 43, 2786-2799.	1.7	0
40	Influence of the Active Screen Plasma Power during Afterglow Nitrocarburizing on the Surface Modification of AISI 316L. Coatings, 2020, 10, 1112.	1.2	9
41	Modeling of the cyclic deformation behavior of austenitic TRIP-steels. International Journal of Plasticity, 2020, 133, 102792.	4.1	13
42	Recycling of carbon fiber composites in carbon-bonded alumina refractories. Ceramics International, 2020, 46, 12574-12583.	2.3	9
43	Impact of Al addition on deformation behavior of Fe–Cr–Ni–Mn–C austenitic stainless steel. Materials Science & Engineering A: Structural Materials: Properties, Microstructure and Processing, 2020, 797, 140084.	2.6	11
44	Neutron diffraction analysis of stress and strain partitioning in a two-phase microstructure with parallel-aligned phases. Scientific Reports, 2020, 10, 13536.	1.6	3
45	Ultrasonic fatigue testing of cast steel G42CrMo4 at elevated temperatures. Fatigue and Fracture of Engineering Materials and Structures, 2020, 43, 2455-2475.	1.7	11
46	Determining the Damage and Failure Behaviour of Textile Reinforced Composites under Combined In-Plane and Out-of-Plane Loading. Materials, 2020, 13, 4772.	1.3	4
47	On the formation of ridges and burnished debris along internal fatigue crack propagation in 42CrMo4 steel. Fatigue and Fracture of Engineering Materials and Structures, 2020, 43, 1567-1582.	1.7	6
48	Microstructural and Mechanical Characterization of Squareâ€Celled TRIP Steel Honeycomb Structures Produced by Electron Beam Melting. Advanced Engineering Materials, 2020, 22, 2000037.	1.6	5
49	Microstructural and mechanical characterization of high-alloy quenching and partitioning TRIP steel manufactured by electron beam melting. Materials Science & Engineering A: Structural Materials: Properties, Microstructure and Processing, 2020, 794, 139684.	2.6	9
50	Solid carbon active screen plasma nitrocarburizing of AISI 316L stainless steel in cold wall reactor: influence of plasma conditions. Journal of Materials Research and Technology, 2020, 9, 9195-9205.	2.6	23
51	Spectroscopic study of plasma nitrocarburizing processes with an industrial-scale carbon active screen. Plasma Sources Science and Technology, 2020, 29, 035001.	1.3	12
52	Crack growth behaviour in biaxial stress fields: Calculation of K-factors for cruciform specimens. Theoretical and Applied Fracture Mechanics, 2020, 107, 102521.	2.1	7
53	Effect of Compositional Variation Induced by EBM Processing on Deformation Behavior and Phase Stability of Austenitic Cr-Mn-Ni TRIP Steel. Jom, 2020, 72, 1052-1064.	0.9	12
54	Scanning Electron Microscopy and Complementary In Situ Characterization Techniques for Characterization of Deformation and Damage Processes. Springer Series in Materials Science, 2020, , 485-527.	0.4	1

#	Article	IF	CITATIONS
55	Cyclic Deformation and Fatigue Behavior of Metastable Austenitic Steels and Steel-Matrix-Composites. Springer Series in Materials Science, 2020, , 413-449.	0.4	0
56	Behaviour of Metastable and Stable Austenitic Stainless Steels Under Planar-Biaxial Load. Springer Series in Materials Science, 2020, , 451-483.	0.4	0
57	Electron Beam Technologies for the Joining of High Alloy TRIP/TWIP Steels and Steel-Matrix Composites. Springer Series in Materials Science, 2020, , 283-323.	0.4	Ο
58	Plasma Nitrocarburizing of AISI 316L Austenitic Stainless Steel: a First Step for Treatment of Components with Complex Geometries. HTM - Journal of Heat Treatment and Materials, 2020, 75, 95-112.	0.1	2
59	Plasma Nitrocarburizing of AISI 316L Austenitic Stainless Steel: a First Step for Treatment of Components with Complex Geometries. HTM - Journal of Heat Treatment and Materials, 2020, 75, 95-112.	0.1	Ο
60	Quality of dissimilar welded particle-reinforced TRIP/TWIP steels generated by electron beam braze-welding. Welding in the World, Le Soudage Dans Le Monde, 2019, 63, 1655-1667.	1.3	1
61	Martensite formation during tensile deformation of high-alloy TRIP steel after quenching and partitioning route investigated by digital image correlation. Materialia, 2019, 8, 100498.	1.3	13
62	Tempering Reactions and Elemental Redistribution During Tempering of Martensitic Stainless Steels. Metallurgical and Materials Transactions A: Physical Metallurgy and Materials Science, 2019, 50, 3663-3673.	1.1	12
63	Electron beam welding of CrMnNi-steels: CFD-modeling with temperature sensitive thermophysical properties. International Journal of Heat and Mass Transfer, 2019, 139, 442-455.	2.5	18
64	TRIPâ€Matrix omposites. Advanced Engineering Materials, 2019, 21, 1900126.	1.6	2
65	Evaluation of very high cycle fatigue zones in 42CrMo4 steel with plate-like alumina inclusions. International Journal of Fatigue, 2019, 126, 258-269.	2.8	13
66	Laminated TRIP/TWIP Steel Composites Produced by Roll Bonding. Metals, 2019, 9, 195.	1.0	8
67	Strain Hardening of Phases in Highâ€Alloy CrMnNi Steel as a Consequence of Preâ€Deformation Studied by Nanoindentation. Advanced Engineering Materials, 2019, 21, 1800801.	1.6	7
68	Electron Beam Welding and Characterization of Dissimilar Joints with TWIP Matrix Composites. Advanced Engineering Materials, 2019, 21, 1800586.	1.6	5
69	Investigation of fatigue crack growth under in-phase loading as well as phase-shifted loading using cruciform specimens. International Journal of Fatigue, 2019, 124, 595-617.	2.8	15
70	Cruciform specimens for the determination of crack growth behaviour in biaxial stress fields: calculation of K-factors. MATEC Web of Conferences, 2019, 300, 11008.	0.1	0
71	Mechanical High-Temperature Properties and Damage Behavior of Coarse-Grained Alumina Refractory Metal Composites. Materials, 2019, 12, 3927.	1.3	13
72	Thermal Analysis of the Formation and Dissolution of Crâ€Rich Carbides in Alâ€Alloyed Stainless Steels. Advanced Engineering Materials, 2019, 21, 1800658.	1.6	8

#	Article	IF	CITATIONS
73	Numerical Simulation of the Particle Displacement during Electron Beam Welding of a Dissimilar Weld Joint with TRIPâ€Matrixâ€Composite. Advanced Engineering Materials, 2019, 21, 1800741.	1.6	3
74	Fatigue Crack Growth in Austenitic Stainless Steel: Effects of Phase Shifted Loading and Crack Paths. Advanced Engineering Materials, 2019, 21, 1800861.	1.6	6
75	Characterization of Nonmetallic Inclusions in 18CrNiMo7-6. Metallurgical and Materials Transactions B: Process Metallurgy and Materials Processing Science, 2019, 50, 337-356.	1.0	7
76	Solid carbon active screen plasma nitrocarburizing of AISI 316L stainless steel: Influence of N2-H2 gas composition on structure and properties of expanded austenite. Surface and Coatings Technology, 2019, 357, 1060-1068.	2.2	27
77	Cyclic Deformation Behavior of an Ultraâ€High Strength Austeniticâ€Martensitic Steel Treated by Novel Q&P Processing. Advanced Engineering Materials, 2019, 21, 1800732.	1.6	4
78	Validation of an experimental-numerical approach for the high temperature behaviour of open-cell ceramic foams. Journal of the European Ceramic Society, 2019, 39, 610-617.	2.8	8
79	Cruciform specimens used for determination of the influence of T-stress on fatigue crack growth with overloads on aluminum alloy Al 6061 T651. Frattura Ed Integrita Strutturale, 2019, 13, 135-143.	0.5	1
80	Comparative Studies on Electron Beam and Laser Beam Welding of QT-Steel and Structural Steel. HTM - Journal of Heat Treatment and Materials, 2019, 74, 331-341.	0.1	1
81	On the effect of internal channels and surface roughness on the high-cycle fatigue performance of Ti-6Al-4V processed by SLM. Materials and Design, 2018, 143, 1-11.	3.3	98
82	Design of novel materials for additive manufacturing - Isotropic microstructure and high defect tolerance. Scientific Reports, 2018, 8, 1298.	1.6	76
83	The influence of the nitrogen/nickelâ€ratio on the cyclic behavior of austenitic high strength steels with twinningâ€induced plasticity and transformationâ€induced plasticity effects. Materialwissenschaft Und Werkstofftechnik, 2018, 49, 61-72.	0.5	3
84	Use of a solid carbon precursor for DC plasma nitrocarburizing of AISI 4140 steel. Vacuum, 2018, 149, 146-149.	1.6	13
85	Investigation of cracking prevention in magnetron-sputtered TiAlN coatings during subsequent electron beam hardening. Surface and Coatings Technology, 2018, 338, 75-83.	2.2	5
86	On the identification of an effective cross section for a cruciform specimen. Strain, 2018, 54, e12257.	1.4	8
87	Influence of particle and short-fibre reinforcement on the very high cycle fatigue behaviour of aluminium matrix composites. International Journal of Fatigue, 2018, 113, 299-310.	2.8	9
88	Fatigue behavior of an ultrafine-grained metastable CrMnNi steel tested under total strain control. International Journal of Fatigue, 2018, 106, 143-152.	2.8	19
89	Development of a novel testing device for fabric reinforced carbon fibre composites under cyclic biaxial load applications. IOP Conference Series: Materials Science and Engineering, 2018, 388, 012019.	0.3	0
90	Very high cycle fatigue behaviour of 42CrMo4 steel with plate-like alumina inclusions. Procedia Structural Integrity, 2018, 13, 2071-2076.	0.3	2

#	Article	IF	CITATIONS
91	On the Potential of Using the Small Punch Test for the Characterization of SMA Behavior Under Multi-Axial Loading Conditions. , 2018, , .		Ο
92	Influence of ceramic particles and fibre reinforcement in metal matrix composites on the VHCF behaviour. Part II: Stochastic modelling and statistical inference. , 2018, , 319-342.		0
93	Joining of TWIP-matrix composites by electron beam brazing. Welding in the World, Le Soudage Dans Le Monde, 2018, 62, 19-27.	1.3	2
94	Cyclic deformation behavior of a damage tolerant CrMnNi TRIP steel produced by electron beam melting. International Journal of Fatigue, 2018, 114, 262-271.	2.8	24
95	Cluster Detection of Nonâ€Metallic Inclusions in 42CrMo4 Steel. Steel Research International, 2018, 89, 1800216.	1.0	11
96	Spectroscopic investigations of plasma nitrocarburizing processes using an active screen made of carbon in a model reactor. Plasma Sources Science and Technology, 2018, 27, 075017.	1.3	10
97	On the influence of carbon contamination of reactor parts in active screen plasma nitrocarburizing processes. Journal of Applied Physics, 2018, 123, .	1.1	9
98	Study of Deformation Phenomena in TRIP/TWIP Steels by Acoustic Emission and Scanning Electron Microscopy. Physics of Metals and Metallography, 2018, 119, 388-395.	0.3	14
99	Influence of Si addition on the carbon partitioning process in martensitic-austenitic stainless steels. IOP Conference Series: Materials Science and Engineering, 2018, 373, 012001.	0.3	6
100	On the origin of subgrain boundaries during conventional solidification of austenitic stainless steels. IOP Conference Series: Materials Science and Engineering, 2018, 373, 012005.	0.3	10
101	Plasma Nitrocarburizing of AISI 316L Austenitic Stainless Steel Applying a Carbon Active Screen: Status and Perspectives. HTM - Journal of Heat Treatment and Materials, 2018, 73, 246-257.	0.1	8
102	Fracture mechanics testing and crack growth simulation of highly ductile austenitic steel. Materialpruefung/Materials Testing, 2018, 60, 341-348.	0.8	7
103	Spectroscopic investigations of plasma nitriding processes using an active screen made of carbon in a model reactor. , 2018, , .		Ο
104	Fatigue life of additively manufactured Ti–6Al–4V in the very high cycle fatigue regime. International Journal of Fatigue, 2017, 94, 236-245.	2.8	321
105	Tensile elongation of lean-alloy austenitic stainless steels: Transformation-induced plasticity versus planar glide. Materials Science and Technology, 2017, 33, 1224-1230.	0.8	10
106	Spectroscopic investigations of plasma nitriding processes: A comparative study using steel and carbon as active screen materials. Journal of Applied Physics, 2017, 121, 153301.	1.1	23
107	Prediction of High Temperature Behavior of Openâ€Cell Ceramic Foams Using an Experimentalâ€Numerical Approach. Advanced Engineering Materials, 2017, 19, 1700082.	1.6	4
108	Fatigue behaviour of 16Mo3 steel at elevated temperatures under uniaxial as well as biaxialâ€planar loading. Fatigue and Fracture of Engineering Materials and Structures, 2017, 40, 909-923.	1.7	6

#	Article	IF	CITATIONS
109	Ductile behavior of fine-grained, carbon-bonded materials at elevated temperatures. Carbon, 2017, 122, 141-149.	5.4	21
110	Impact of Nanoengineered Surfaces of Carbonâ€Bonded Alumina Filters on Steel Cleanliness. Advanced Engineering Materials, 2017, 19, 1700153.	1.6	13
111	Effect of Crucible Material for Ingot Casting on Detrimental Nonâ€Metallic Inclusions and the Resulting Mechanical Properties of 18CrNiMo7â€6 Steel. Advanced Engineering Materials, 2017, 19, 1700199.	1.6	14
112	lsothermal and thermo-mechanical fatigue behavior of 16Mo3 steel coated with high-velocity oxy-fuel sprayed nickel-base alloy under uniaxial as well as biaxial-planar loading. Journal of Materials Research, 2017, 32, 4411-4423.	1.2	7
113	Dilatometry Analysis of Dissolution of Cr-Rich Carbides in Martensitic Stainless Steels. Metallurgical and Materials Transactions A: Physical Metallurgy and Materials Science, 2017, 48, 5771-5777.	1.1	19
114	Cyclic Degradation Behavior of \$\$ langle 001 angle \$\$ âŸ [.] 001 ⟩ -Oriented Fe–Mn–Al–Ni Single Crystals in Tension. Shape Memory and Superelasticity, 2017, 3, 335-346.	1.1	22
115	A new method for manufacturing graded refractories by localized hot uniaxial pressing. Ceramics International, 2017, 43, 14636-14641.	2.3	3
116	Crack initiation in the very high cycle fatigue regime of nitrided 42CrMo4 steel. Journal of Materials Research, 2017, 32, 4305-4316.	1.2	13
117	Electron beam welding of Fe–Mn–Al–Ni shape memory alloy: Microstructure evolution and shape memory response. Functional Materials Letters, 2017, 10, 1750043.	0.7	14
118	Spectroscopic investigations of plasma nitriding processes: A comparative study using steel and carbon as active screen materials. , 2017, , .		0
119	Investigations of Electron Beam Hardening on TiAlN Coated Heat-Ã,"Treatable Steel. Materials Performance and Characterization, 2017, 6, 850-859.	0.2	1
120	A Novel Approach of Plasma Nitrocarburizing Using a Solid Carbon Active Screen – a Proof of Concept. HTM - Journal of Heat Treatment and Materials, 2017, 72, 254-259.	0.1	19
121	Electron Beam Welding of Cold Rolled Highâ€Alloy TRIP/TWIP Steel Sheets. Steel Research International, 2016, 87, 436-444.	1.0	13
122	Application of a Modified Stressâ^'Strain Approach for the Fatigueâ€Life Prediction of a Ferritic, an Austenitic and a Ferritic–Austenitic Duplex Steel under Isothermal and Thermoâ€Mechanical Fatigue. Steel Research International, 2016, 87, 1095-1104.	1.0	3
123	Tensile Behavior of Cast and Electron Beam Welded Interstitially Strengthened High-Alloy TRIP Steel. Steel Research International, 2016, 87, 1627-1637.	1.0	2
124	Highâ€Temperature Compression Deformation Behavior of Fineâ€Grained Carbonâ€Bonded Alumina. Journal of the American Ceramic Society, 2016, 99, 1390-1397.	1.9	14
125	Microstructure of Nonâ€Metallic Inclusions Identified in Cast Steel 42CrMo4 after Metal Melt Filtration by Novel Foam Filters. Steel Research International, 2016, 87, 1038-1053.	1.0	12
126	The influence of dilution on dissimilar weld joints with high-alloy TRIP/TWIP steels. Welding in the World, Le Soudage Dans Le Monde, 2016, 60, 645-652.	1.3	19

#	Article	IF	CITATIONS
127	Decomposition and Precipitation Process During Thermo-mechanical Fatigue of Duplex Stainless Steel. Metallurgical and Materials Transactions A: Physical Metallurgy and Materials Science, 2016, 47, 2112-2124.	1.1	6
128	Microstructural Evolution and Functional Properties of Fe-Mn-Al-Ni Shape Memory Alloy Processed by Selective Laser Melting. Metallurgical and Materials Transactions A: Physical Metallurgy and Materials Science, 2016, 47, 2569-2573.	1.1	50
129	Volumetric changes associated with B2-(Ni,Fe)Al dissolution in an Al-alloyed ferritic steel. Materials and Design, 2016, 111, 640-645.	3.3	12
130	Investigation of isothermal and thermo-mechanical fatigue behavior of the nickel-base superalloy IN738LC using standardized and advanced test methods. Materials Science & Engineering A: Structural Materials: Properties, Microstructure and Processing, 2016, 670, 314-324.	2.6	28
131	Small-scale specimen testing for fatigue life assessment of service-exposed industrial gas turbine blades. International Journal of Fatigue, 2016, 92, 262-271.	2.8	48
132	Microstructural Evolution of an Al-Alloyed Duplex Stainless Steel During Tensile Deformation Between 77 K and 473 K (Ⱂ196°C and 200°C). Metallurgical and Materials Transactions A: Physical Metallurgy and Materials Science, 2016, 47, 2705-2716.	1.1	12
133	Influence of Martensite Fraction on Tensile Properties of Quenched and Partitioned (Q&P) Martensitic Stainless Steels. Steel Research International, 2016, 87, 1082-1094.	1.0	33
134	Influence of non-metallic inclusions on fatigue life in the very high cycle fatigue regime. International Journal of Fatigue, 2016, 84, 40-52.	2.8	75
135	Influence of Martensite Fraction on the Stabilization of Austenite in Austenitic–Martensitic Stainless Steels. Metallurgical and Materials Transactions A: Physical Metallurgy and Materials Science, 2016, 47, 1947-1959.	1.1	24
136	Cyclic degradation in bamboo-like Fe–Mn–Al–Ni shape memory alloys — The role of grain orientation. Scripta Materialia, 2016, 114, 156-160.	2.6	61
137	Influence of Al on the temperature dependence of strain hardening behavior and glide planarity in Fe–Cr–Ni–Mn–C austenitic stainless steels. Materials Science & Engineering A: Structural Materials: Properties, Microstructure and Processing, 2016, 649, 301-312.	2.6	31
138	Functionally Graded High-Alloy CrMnNi TRIP Steel Produced by Local Heat Treatment Using High-Energy Electron Beam. Metallurgical and Materials Transactions A: Physical Metallurgy and Materials Science, 2016, 47, 123-138.	1.1	2
139	Investigation of Phase Transformations in High-Alloy Austenitic TRIP Steel Under High Pressure (up to) Tj ETQq1 Materials Transactions A: Physical Metallurgy and Materials Science, 2016, 47, 95-111.	1 0.784314 1.1	4 rgBT /Ovei 27
140	The Portevin–Le Châtelier Effect in a Metastable Austenitic Stainless Steel. Metallurgical and Materials Transactions A: Physical Metallurgy and Materials Science, 2016, 47, 59-74.	1.1	31
141	Influence of Temperature on Fatigue-Induced Martensitic Phase Transformation in a Metastable CrMnNi-Steel. Metallurgical and Materials Transactions A: Physical Metallurgy and Materials Science, 2016, 47, 84-94.	1.1	18
142	In-line Process Control in the Active Screen Plasma Nitrocarburizing Using a Combined Approach Based on Infrared Laser Absorption Spectroscopy and Bias Power Management*. HTM - Journal of Heat Treatment and Materials, 2016, 71, 141-147.	0.1	11
143	Crack growth behavior of aluminum alloy 6061 T651 under uniaxial and biaxial planar testing condition. Frattura Ed Integrita Strutturale, 2016, , .	0.5	1
144	Biaxial fatigue behavior of a powder metallurgical TRIP steel. Frattura Ed Integrita Strutturale, 2016, , .	0.5	3

#	Article	IF	CITATIONS
145	Portevin Le Chatelier Effect in a Metastable Austenitic CrMnNi Steel. Materials Today: Proceedings, 2015, 2, S623-S626.	0.9	1
146	Texture evolution of cold rolled and reversion annealed metastable austenitic CrMnNi steels. IOP Conference Series: Materials Science and Engineering, 2015, 82, 012069.	0.3	4
147	Electron beam hardening of PVD-coated steels — Improved load-supporting capacity for Ti1â^'xAlxN layers. Surface and Coatings Technology, 2015, 283, 201-209.	2.2	7
148	Magnitude of shear of deformation-induced α′-martensite in high-alloy metastable steel. Materials Letters, 2015, 143, 155-158.	1.3	23
149	Deformation and strain hardening behavior of powder metallurgical TRIP steel under quasi-static biaxial-planar loading. Materials Science & Engineering A: Structural Materials: Properties, Microstructure and Processing, 2015, 642, 317-329.	2.6	27
150	Case studies on the application of high-resolution electron channelling contrast imaging – investigation of defects and defect arrangements in metallic materials. Philosophical Magazine, 2015, 95, 759-793.	0.7	28
151	Application of full-surface view in situ thermography measurements during ultrasonic fatigue of cast steel G42CrMo4. International Journal of Fatigue, 2015, 80, 459-467.	2.8	30
152	On the effect of gamma phase formation on the pseudoelastic performance of polycrystalline Fe–Mn–Al–Ni shape memory alloys. Scripta Materialia, 2015, 108, 23-26.	2.6	92
153	Isothermal and thermo-mechanical fatigue behavior of the nickel base superalloy Waspaloyâ,,¢ under uniaxial and biaxial-planar loading. International Journal of Fatigue, 2015, 81, 21-36.	2.8	31
154	Combination of Different In Situ Characterization Techniques and Scanning Electron Microscopy Investigations for a Comprehensive Description of the Tensile Deformation Behavior of a CrMnNi TRIP/TWIP Steel. Jom, 2015, 67, 1729-1747.	0.9	34
155	Fatigue crack initiation and damage mechanisms during ultrasonic fatigue testing of cast aluminium alloy AlSi7Mg. MATEC Web of Conferences, 2014, 12, 10005.	0.1	4
156	Duplex Surface Treatment – Physical Vapor Deposition (PVD) and Subsequent Electron Beam Hardening (EBH). Advanced Engineering Materials, 2014, 16, 511-516.	1.6	21
157	Numerical and Experimental Sensitivity Analysis for the Determination of Casting Parameter–Microstructure–Property Relations and Mechanical Properties of IN738LC in Investment Casting. Advanced Engineering Materials, 2014, 16, 1217-1225.	1.6	1
158	Progress in control of nitriding potential in ASPN process. International Heat Treatment and Surface Engineering, 2014, 8, 139-143.	0.2	10
159	Fatigue behaviour of hot pressed austenitic TWIP steel and TWIP steel/Mg-PSZ composite materials. International Journal of Fatigue, 2014, 65, 9-17.	2.8	22
160	Effects of electron beam treatment on Ti(1â^'x)AlxN coatings on steel. Vacuum, 2014, 107, 141-144.	1.6	10
161	Biaxial in-phase and out-of-phase cyclic deformation and fatigue behavior of an austenitic TRIP steel. International Journal of Fatigue, 2014, 67, 123-133.	2.8	31
162	Thermo mechanical fatigue behaviour of a duplex stainless steel in the range of 350–600°C. International Journal of Fatigue, 2014, 65, 2-8.	2.8	7

#	Article	IF	CITATIONS
163	Deformation mechanisms in austenitic TRIP/TWIP steels at room and elevated temperature investigated by acoustic emission and scanning electron microscopy. Materials Science & Engineering A: Structural Materials: Properties, Microstructure and Processing, 2014, 597, 183-193.	2.6	57
164	Nanoindentation measurements on deformation-induced α'-martensite in a metastable austenitic high-alloy CrMnNi steel. Philosophical Magazine Letters, 2014, 94, 522-530.	0.5	39
165	Microstructure and mechanical properties of Al-alloyed Fe–Cr–Ni–Mn–C stainless steels. Materials Science & Engineering A: Structural Materials: Properties, Microstructure and Processing, 2014, 618, 46-55.	2.6	24
166	IFHTSE Global 21: heat treatment and surface engineering in the twenty-first century Active screen plasma nitriding and nitrocarburising of steels: an overview. International Heat Treatment and Surface Engineering, 2014, 8, 94-106.	0.2	17
167	High-temperature small punch test for mechanical characterization of a nickel-base super alloy. Materials Science & Engineering A: Structural Materials: Properties, Microstructure and Processing, 2014, 613, 259-263.	2.6	18
168	Fatigue behavior of the nickel-base superalloy Waspaloyâ"¢ under proportional biaxial-planar loading at high temperature. International Journal of Fatigue, 2014, 67, 212-219.	2.8	20
169	Strength of fine grained carbon-bonded alumina (Al2O3–C) materials obtained by means of the small punch test. Ceramics International, 2014, 40, 9555-9561.	2.3	16
170	Scanning and transmission electron microscopy investigations of defect arrangements in a two-phase Î ³ -TiAl alloy. Materials Science & Engineering A: Structural Materials: Properties, Microstructure and Processing, 2013, 571, 49-56.	2.6	7
171	Influence of Matrix Strength and Volume Fraction of Mg‫scp>PSZ on the Cyclic Deformation Behavior of Hot Pressed <scp>TRIP</scp> / <scp>TWIP</scp> ‫scp>Matrix Composite Materials. Advanced Engineering Materials, 2013, 15, 550-557.	1.6	9
172	Application of in situ thermography for evaluating the high-cycle and very high-cycle fatigue behaviour of cast aluminium alloy AlSi7Mg (T6). Ultrasonics, 2013, 53, 1441-1449.	2.1	38
173	Microstructure and mechanical properties of fine grained carbon-bonded Al 2 O 3 –C materials. Ceramics International, 2013, 39, 6695-6702.	2.3	16
174	Determination of stretch zone width and height by powerful 3D SEM imaging technology. Engineering Fracture Mechanics, 2013, 108, 294-304.	2.0	24
175	Kinetics of deformation processes in high-alloyed cast transformation-induced plasticity/twinning-induced plasticity steels determined by acoustic emission and scanning electron microscopy: Influence of austenite stability on deformation mechanisms. Acta Materialia, 2013, 61, 2434-2449.	3.8	91
176	Ultrafine grained high-alloyed austenitic TRIP steel. Materials Science & Engineering A: Structural Materials: Properties, Microstructure and Processing, 2013, 571, 68-76.	2.6	45
177	Thermodynamicâ€ <scp>M</scp> echanical Modeling of Strainâ€ <scp>I</scp> nduced α′â€ <scp>M</scp> arter Formation in Austenitic Cr– <scp>M</scp> n– <scp>N</scp> i Asâ€ <scp>C</scp> ast Steel. Advanced Engineering Materials, 2013, 15, 609-617.	nsite 1.6	13
178	Deformation and microstructure evolution of a duplex stainless steel under out-of-phase thermo-mechanical fatigue. Materials at High Temperatures, 2013, 30, 77-82.	0.5	6
179	<i>In Situ</i> Tensile Deformation of TRIP Steel / Mg-PSZ Composites. Materials Science Forum, 2013, 738-739, 77-81.	0.3	11
180	Influence of Composition and Coking Temperature on the Properties and Microstructure of Carbon Bonded Al ₂ <scp>O</scp> ₃ – <scp>C</scp> Filter Materials. Advanced Engineering Materials, 2013, 15, 1224-1229.	1.6	14

#	Article	IF	CITATIONS
181	Effect of Filter Coating on the Quasiâ€ <scp>S</scp> tatic and Cyclic Mechanical Properties of a G42 <scp>C</scp> r <scp>M</scp> o4 Casting. Advanced Engineering Materials, 2013, 15, 1216-1223.	1.6	15
182	Investigation of the Damage Behavior of Cast Steel 42 <scp>C</scp> r <scp>M</scp> o4 During Ultrasonic Fatigue by Combination of Thermography and Fractography. Advanced Engineering Materials, 2013, 15, 1251-1259.	1.6	13
183	Electron Beam Welding of High Alloy CrMnNi Cast Steels with TRIP/TWIP Effect. Advanced Engineering Materials, 2013, 15, 566-570.	1.6	14
184	Influence of the Chemistry of Surface Functionalized Ceramic Foam Filters on the Filtration of Alumina Inclusions in Steel Melts. Advanced Engineering Materials, 2013, 15, 1188-1196.	1.6	31
185	Kontrolliertes Plasmanitrieren von StĤlen mit einem Aktivgitter. HTM - Journal of Heat Treatment and Materials, 2013, 68, 124-132.	0.1	8
186	Optical in situ investigations of overload effects during fatigue crack growth in nodular cast iron. Engineering Fracture Mechanics, 2012, 95, 45-56.	2.0	17
187	Influence of graphite spherical size on fatigue behaviour and fracture toughness of ductile cast iron EN-GJS-400-18LT. International Journal of Materials Research, 2012, 103, 87-96.	0.1	19
188	Static and Cyclic Deformation Behavior of the Ferritic Steel 16Mo3 Under Monotonic and Cyclic Loading at High Temperatures. Steel Research International, 2012, 83, 631-636.	1.0	7
189	Cyclic Deformation of Powder Metallurgy Stainless Steel/Mgâ€PSZ Composite Materials. Steel Research International, 2012, 83, 554-564.	1.0	20
190	SEM Investigation of Highâ€Alloyed Austenitic Stainless Cast Steels With Varying Austenite Stability at Room Temperature and 100°C. Steel Research International, 2012, 83, 512-520.	1.0	50
191	Thermo-mechanical fatigue behaviour of a duplex stainless steel. International Journal of Fatigue, 2012, 37, 86-91.	2.8	16
192	In-situ monitoring of plasma enhanced nitriding processes using infrared absorption and mass spectroscopy. Surface and Coatings Technology, 2012, 206, 3955-3960.	2.2	33
193	Erhöhung der tribologischen Beanspruchbarkeit von Aluminiumwerkstoffen durch die Kombination von Randschichtumschmelzlegieren und Nitrieren. HTM - Journal of Heat Treatment and Materials, 2012, 67, 13-21.	0.1	1
194	Microstructure of austenitic stainless steels of various phase stabilities after cyclic and tensile deformation. International Journal of Materials Research, 2011, 102, 1374-1377.	0.1	14
195	Stacking faults in high-alloyed metastable austenitic cast steel observed by electron channelling contrast imaging. Scripta Materialia, 2011, 64, 513-516.	2.6	89
196	Characterization of stress–strain behavior of a cast TRIP steel under different biaxial planar load ratios. Engineering Fracture Mechanics, 2011, 78, 1684-1695.	2.0	70
197	The Effect of Weld Profile and Geometries of Butt Weld Joints on Fatigue Life Under Cyclic Tensile Loading. Journal of Materials Engineering and Performance, 2011, 20, 1385-1391.	1.2	15
198	Cyclic Deformation Behaviour of Three Austenitic Cast CrMnNi TRIP/TWIP Steels with Various Ni Content. Steel Research International, 2011, 82, 1040-1047.	1.0	55

#	Article	IF	CITATIONS
199	Microstructure and Local Strain Fields in a Highâ€Alloyed Austenitic Cast Steel and a Steelâ€Matrix Composite Material after in situ Tensile and Cyclic Deformation. Steel Research International, 2011, 82, 990-997.	1.0	16
200	Biaxial Low Cycle Fatigue Behavior and Martensite Formation of a Metastable Austenitic Cast TRIP Steel Under Proportional Loading. Steel Research International, 2011, 82, 1141-1148.	1.0	15
201	Editorial TRIPâ€Matrix Composites. Steel Research International, 2011, 82, 983-984.	1.0	0
202	Investigation of Stress Induced Phase Transformation in TRIPâ€&teel/Mgâ€PSZ Composites Using EBSD. Advanced Engineering Materials, 2011, 13, 1037-1041.	1.6	5
203	Mechanical properties of metal matrix composites based on TRIP steel and ZrO2 ceramic foams. Procedia Engineering, 2011, 10, 548-555.	1.2	6
204	Stability of austenitic 316L steel against martensite formation during cyclic straining. Procedia Engineering, 2011, 10, 1279-1284.	1.2	39
205	Observation of stacking faults in a scanning electron microscope by electron channelling contrast imaging. International Journal of Materials Research, 2011, 102, 3-5.	0.1	17
206	Untersuchungen zum Plasmanitrieren von StÄ ¤ len mit einem Aktivgitter*. HTM - Journal of Heat Treatment and Materials, 2011, 66, 127-134.	0.1	3
207	Thermo-mechanical fatigue behavior of the intermetallic gamma-TiAl alloy TNB-V5 with different microstructures. Journal of Physics: Conference Series, 2010, 240, 012046.	0.3	1
208	Thermomechanical Fatigue Behavior of the Intermetallic Î ³ -TiAl Alloy TNB-V5 with Different Microstructures. Metallurgical and Materials Transactions A: Physical Metallurgy and Materials Science, 2010, 41, 717-726.	1.1	11
209	Comparison of the Stress Intensity Factor of Load-Carrying Cruciform Welded Joints with Different Geometries. Journal of Materials Engineering and Performance, 2010, 19, 802-809.	1.2	23
210	Determination of Some Parameters for Fatigue Life in Welded Joints Using Fracture Mechanics Method. Journal of Materials Engineering and Performance, 2010, 19, 1225-1234.	1.2	29
211	Novel TRIP‧teel/Mgâ€PSZ Composite–Open Cell Foam Structures for Energy Absorption. Advanced Engineering Materials, 2010, 12, 197-204.	1.6	36
212	Influence of overloads on the fatigue crack growth in nodular cast iron: experiments and numerical simulation. Procedia Engineering, 2010, 2, 1557-1567.	1.2	14
213	In-situ characterization of the microstructure evolution during cyclic deformation of novel cast TRIP steel. Procedia Engineering, 2010, 2, 1961-1971.	1.2	36
214	Effect of austenite stability on the low cycle fatigue behavior and microstructure of high alloyed metastable austenitic cast TRIPsteels. Procedia Engineering, 2010, 2, 2085-2094.	1.2	66
215	Crack observation methods, their application and simulation of curved fatigue crack growth. Engineering Fracture Mechanics, 2010, 77, 2077-2090.	2.0	24
216	Low-cycle fatigue behaviour and microstructure of copper and alpha-brass under biaxial load paths. Journal of Physics: Conference Series, 2010, 240, 012042.	0.3	3

#	Article	IF	CITATIONS
217	Corrosion behaviour of stainless steels after low temperature thermochemical treatment. Materialwissenschaft Und Werkstofftechnik, 2010, 41, 133-141.	0.5	18
218	Microstructure and Compression Strength of Novel TRIP‣teel/Mgâ€PSZ Composites. Advanced Engineering Materials, 2009, 11, 1000-1006.	1.6	31
219	Energyâ€Absorbing TRIPâ€Steel/Mgâ€PSZ Composite Honeycomb Structures Based on Ceramic Extrusion at Room Temperature. International Journal of Applied Ceramic Technology, 2009, 6, 727-735.	1.1	57
220	Collaborative Research Center TRIP-Matrix-Composite. , 2009, , .		4
221	Low cycle fatigue behavior and microstructure of a high alloyed metastable austenitic cast TRIP-steel. , 2009, , .		4
222	Thermo-mechanical fatigue behaviour of a modern Î ³ -TiAl alloy. International Journal of Fatigue, 2008, 30, 352-356.	2.8	30
223	Untersuchung des Korrosionsverhaltens von nichtrostenden StÄ ¤ len nach einer thermochemischen Behandlung bei tiefen Temperaturen. HTM - Journal of Heat Treatment and Materials, 2008, 63, 342-350.	0.1	6
224	Thermo-Mechanical Fatigue Behaviour of the Gamma-Titanium Aluminide TNB-V5 with Near-Gamma Microstructure. Materials Science Forum, 2007, 539-543, 1559-1564.	0.3	1
225	Load history effects in ductile cast iron for wind turbine components. International Journal of Fatigue, 2007, 29, 1788-1796.	2.8	45
226	Mechanical Behavior and Fatigue Properties of Metal-matrix Composites. , 2006, , 173-196.		1
227	Estimation of the effective properties of particle-reinforced metal–matrix composites from microtomographic reconstructions. Acta Materialia, 2006, 54, 2735-2744.	3.8	46
228	Thermo-mechanical fatigue behaviour of the γ-TiAl alloy TNB-V5. Scripta Materialia, 2006, 54, 137-141.	2.6	27
229	Nitriding behaviour of the intermetallic alloy FeAl. International Journal of Materials Research, 2005, 96, 781-786.	0.8	14
230	Microstructure based three-dimensional finite element modeling of particulate reinforced metal–matrix composites. Materials Science & Engineering A: Structural Materials: Properties, Microstructure and Processing, 2004, 387-389, 852-856.	2.6	28
231	Fatigue Behaviour of Al-Matrix Composites. Advanced Engineering Materials, 2004, 6, 477-485.	1.6	18
232	Three-dimensional characterization of the microstructure of a metal–matrix composite by holotomography. Materials Science & Engineering A: Structural Materials: Properties, Microstructure and Processing, 2004, 367, 40-50.	2.6	82
233	Low cycle fatigue crack growth and life prediction of short-fibre reinforced aluminium matrix composites. International Journal of Fatigue, 2003, 25, 209-220.	2.8	22
234	The influence of the free surface on the fracture of alumina particles in an Al–Al2O3 metal–matrix composite. Computational Materials Science, 2003, 26, 183-188.	1.4	17

#	Article	IF	CITATIONS
235	Modelling low-cycle fatigue life of particulate-reinforced metal-matrix composites. Materials Science & Engineering A: Structural Materials: Properties, Microstructure and Processing, 2002, 333, 295-305.	2.6	31
236	A low cycle fatigue model of a short-fibre reinforced 6061 aluminium alloy metal matrix composite. Composites Science and Technology, 2002, 62, 2189-2199.	3.8	42
237	Influence of reinforcement morphology and matrix strength of metal?matrix composites on the cyclic deformation and fatigue behaviour. International Journal of Fatigue, 2002, 24, 215-221.	2.8	18
238	On the temperature dependence of the fatigue and damage behaviour of a particulate-reinforced metal-matrix composite. Materials Science & Engineering A: Structural Materials: Properties, Microstructure and Processing, 2001, 319-321, 671-674.	2.6	21
239	FE investigation of the effect of particle distribution on the uniaxial stress–strain behaviour of particulate reinforced metal-matrix composites. Materials Science & Engineering A: Structural Materials: Properties, Microstructure and Processing, 2001, 313, 34-45.	2.6	72
240	A statistical model of fatigue damage evolution in particulate-reinforced metal-matrix-composites. Fatigue and Fracture of Engineering Materials and Structures, 2000, 23, 847-858.	1.7	5
241	Cyclic stress-strain and fatigue behaviour of particulate-reinforced Al-matrix composites. , 1998, , 431-436.		7
242	Low-cycle fatigue of a metal-matrix composite: Influence of pre-straining on the fatigue life. Materials Science & Engineering A: Structural Materials: Properties, Microstructure and Processing, 1997, 234-236, 198-201.	2.6	4
243	MMC aus TRIP-Stahl und MgO Teilstabilisiertem ZrO2 Durch Bildsame Formgebung. , 0, , 147-154.		2
244	EB Surface Alloying and Plasma Nitriding of Different Al Alloys. Materials Science Forum, 0, 690, 91-94.	0.3	13
245	Stress Induced Phase Transformations in TRIP-Steel / Mg-PSZ Composites. Solid State Phenomena, 0, 172-174, 709-714.	0.3	6
246	Microstructure Evolution and Phase Transformation in a Novel High-Alloyed TRIP Steel Observed during <i>in-Situ</i> Tensile and Cyclic Deformation. Key Engineering Materials, 0, 465, 350-353.	0.4	4
247	Kinetics of Deformation Processes in a High-Alloy Cast TWIP Steel Determined by Acoustic Emission and Scanning Electron Microscopy. Key Engineering Materials, 0, 592-593, 489-492.	0.4	1
248	A Comparative Study on Infrared Thermography during Ultrasonic Fatigue Testing of Cast Steel 42CrMo4 and Cast Aluminium Alloy AlSi7Mg. Key Engineering Materials, 0, 592-593, 501-504.	0.4	1
249	Influence of Reinforcement Geometry on the Very High-Cycle Fatigue Behavior of Aluminium-Matrix-Composites. Materials Science Forum, 0, 825-826, 150-157.	0.3	3
250	Influence of Mg-PSZ Particle Size on the Fatigue Behaviour of a High Alloy Steel Matrix Composite. Materials Science Forum, 0, 825-826, 176-181.	0.3	3
251	Microstructure and adhesion characteristics of duplex coatings with different plasmaâ€nitrided layers and a Crâ€Alâ€Tiâ€Bâ€N physical vapor deposition coating. Engineering Reports, 0, , e12364.	0.9	2
252	Residual properties of carbonâ€bonded alumina foam filter coated with carbonâ€containing calcium aluminate after contact with steel melt. Advanced Engineering Materials, 0, , 2100642.	1.6	0

#	Article	IF	CITATIONS
253	Compression Behavior of Carbonâ€Bonded Alumina Spaghetti Filters at Room and High Temperatures. Advanced Engineering Materials, 0, , 2100613.	1.6	1